SCIENCE CHINA
Earth Sciences

•ARTICLE•

May 2024 Vol.67 No.5: 1489–1499
https://doi.org/10.1007/s11430-022-1282-x

Human activity over natural inputs determines the bacterial community in an ice core from the Muztag ata glacier

Yongqin LIU[1,2,3*], Nianzhi JIAO[4], Mukan JI[2], Keshao LIU[1], Baiqing XU[1,3], Bixi GUO[1] & Tandong YAO[1,2,3]

[1] *State Key Laboratory of Tibetan Plateau Earth System, Resources and Environment (TPESRE), Institute of Tibetan Plateau Research, Chinese Academy of Sciences, Beijing 100101, China;*
[2] *Center for Pan-third Pole Environment, Lanzhou University, Lanzhou 730013, China;*
[3] *University of Chinese Academy of Sciences, Beijing 100101, China;*
[4] *State Key Laboratory for Marine Environmental Science, Xiamen University, Xiamen 361102, China*

Received October 18, 2022; revised December 29, 2023; accepted February 22, 2024; published online April 11, 2024

Abstract Ice core provides a valuable vertical timeline of past climates and anthropogenic activities. Environmental proxies have been widely used in these studies, but there are few biological indicators available. To address this gap, we investigated the bacterial community from a 74 m ice core of Muztag ata glacier on the Tibetan Plateau to link biological indicators with past climate and anthropogenic activities. By analyzing the portion of the ice core with environmental proxies available (corresponding to 1907 to 1991), we observed an increase in bacterial richness throughout the ice core, which was associated with higher NH_4^+, an indicator of agricultural development. The bacterial community was jointly determined by human activity, natural input, and air temperature, with a strong human influence after the 1950s. Furthermore, the relative abundance of animal gut-associated bacteria, including *Aerococcaceae*, *Nocardiaceae*, *Muribaculaceae*, and *Lachnospiraceae*, was associated with livestock number changes in the Central Asian region. Together with other bacterial lineages, they jointly explained 59.8% of the livestock number changes. This study provides quantitative evidence of the associations between bacterial indicators and past climate and human activities, highlighting the potential of using bacterial proxies for ice core studies.

Keywords Ice core of Muztag ata glacier, Climate change and anthropogenic activity, Biological indicator, Gut-associated bacteria, livestock number in the Central Asian region

Citation: Liu Y, Jiao N, Ji M, Liu K, Xu B, Guo B, Yao T. 2024. Human activity over natural inputs determines the bacterial community in an ice core from the Muztag ata glacier. Science China Earth Sciences, 67(5): 1489–1499, https://doi.org/10.1007/s11430-022-1282-x

1. Introduction

Ice cores offer a vertical timeline of past climates and anthropogenic activities. The utilization of environmental proxies in ice core studies is widely recognized, such as Ca^{2+} as a proxy for soil dust (Legrand and Mayewski, 1997), $\delta^{18}O$ of water as a proxy for air temperature and precipitation (Yao et al., 2017), while black carbon as a proxy for fossil fuel combustion (McConnell et al., 2007). The application of these proxies in ice core studies has greatly improved our understanding of past climate changes. In addition to environmental proxies, microorganisms as biological proxies are also incorporated into ice core studies (Price and Bay, 2012; Zhang et al., 2017). Ice core microorganisms are mainly bacteria, which were deposited on glacier surface via wet and dry depositions (Qi et al., 2022). Then, they were frozen in ice following post-depositional selection, including *in situ* cell growth and environmental filtering (such as UV radiation and low temperature) (Anesio et al., 2017). The ice core bacterial community has been used to indicate tem-

* Corresponding author (email: yqliu@itpcas.ac.cn)

perature changes and dust events, which provides important supplementary information for interpreting past climates and anthropogenic changes (Yao et al., 2008).

Several studies successfully linked features of the bacterial community in ice cores to past climates, such as dust, temperature, and nutrient availability (Yao et al., 2006; Miteva et al., 2009; Santibáñez et al., 2018). For instance, the differences in bacterial community structure across the depths of the ice core were explained by the climate conditions when bacteria were deposited (Zhang et al., 2008); dust is widely accepted as the principal source of bacteria in ice cores, with a positive correlation between Ca^{2+} and bacterial abundance and diversity being frequently reported (Zhang et al., 2017). In addition to natural input, anthropogenic activity, such as industrialization, can homogenize bacterial communities in geographically separated ice cores (Liu et al., 2016). Nevertheless, previous studies have mostly adopted a quantitative approach, with only the diversity and overall community structure metrics being used. Bacterial taxonomy composition is a crucial attribute of the community, which is distinct among bacterial communities from different habitats (such as deserts, grassland, cities, and marine sources), and is sensitive to ecosystem changes (da C Jesus et al., 2009). As glacier bacteria are transported from distant and regional sources, the ecosystem changes of the source region should also affect the taxonomic composition of the bacteria transported and deposited on the glacier surface. Therefore, we suggest that bacterial lineages could indicate past climate changes and human activities, providing additional insights into the ecosystem changes that typical chemical proxies are unable to offer.

The Tibetan Plateau (TP) has the third-largest number of glaciers after the Antarctic and Greenland. Several ice cores have been drilled from the Tibetan Plateau, providing evidence of historical changes in air temperatures, precipitation (Tian et al., 2006), and anthropogenic activities (Zhao et al., 2011, Wang et al., 2015). The ice core from the Muztag ata glacier, which locates in the west-northern of the Tibetan Plateau, has been intensively studied. Environmental proxies including soluble ions, $\delta^{18}O$ (Zhao et al., 2011), black carbon, and levoglucosan (Wang et al., 2015) have been quantified. However, biological indicators have been poorly investigated. Investigating bacterial diversity, taxonomic composition, and community structure in the ice core provides an opportunity to link biological indicators with past climate, ecosystems, and human activities. This could further enhance our understanding of biological proxies in the ice core. Additionally, the extremely low air temperature (below 0°C) at over 6000 m above sea level (a.s.l.) (Li et al., 2004) inhibits the growth of deposited microorganisms, thereby reducing bacterial community variations due to post-depositional growth. As the bacteria in the ice core are sourced from both distant and local ecosystems, and are impacted by global climate change and anthropogenic activities, this will affect the bacteria deposited on the glacial surface and those frozen in the ice core. Thus, we hypothesize that bacterial community changes across the ice core are consistent with past climate change, and bacterial proxies may indicate features of past climate change that classical geochemical proxies could not.

2. Materials and methods

2.1 Studied area and ice core drilling

Mt. Muztagh ata is located on the eastern Pamir Plateau, Central Asia (38°17'N, 75°06'E, 7546 m), with its precipitation being influenced by the year-round westerly circulation (Wang et al., 2015). In the summer of 2002, a 74 m ice core (9.5 cm in diameter) was drilled using an electromechanical drill without drilling fluid at the elevation of 6300 m from the accumulation zone of Muztagh ata glacier (Figure 1). The ice core was transported frozen (−20°C) to the State Key Laboratory of Cryospheric Science in Lanzhou and processed in a clean −20°C cold room. The ice core was split lengthwise into halves. Half of the ice core was cut into 10–15 cm long sections with approximately 1 cm of the outer annulus removed using a sterilized fine-tooth knife to avoid any possible contamination.

2.2 Environmental proxy measurements and ice core dating

The ice core in the present study has been dated based on the seasonal variations in $\delta^{18}O$ in Wang et al. (2015). Briefly, the dating of ice was based on the seasonal variations in $\delta^{18}O$ as the precipitation $\delta^{18}O$ on the northern Tibetan Plateau exhibits a seasonal cycle with high values in the summer and low values in the winter (Yao et al., 2013). The most recent layer in the Muztag ata ice core was dated to AD 2000, then the rest ice core was dated accordingly (Appendix Figure S1, https://link.springer.com). Dissolved organic carbon (DOC) and Total nitrogen (TN) concentrations were determined using an automated total organic carbon analyzer (TOC-Vcph, Shimadzu, Japan) following the standard methods. The quantification of stable isotopic ratios ($\delta^{18}O$), refractory black carbon (rBC), levoglucosan, as well as soluble ions including SO_4^{2-}, NH_4^+, NO_3^-, Na^+, K^+, Mg^{2+}, Ca^{2+}, Cl^- have been reported previously (Zhao et al., 2011; Wang et al., 2015). Mean annual precipitation (MAP) was downloaded from the Climatic Research Unit (CRU.TS4.04 https://crudata.uea.ac.uk/cru/data/hrg/cru_ts_4.04/cruts.2004151855.v4.04/) covering the period 1901–2000. In addition, data on cattle and sheep numbers in the Central Asian regions were downloaded from the Russian Agricultural Statistics at https://www.ier.hit-u.ac.jp/rrc/English/pdf/RRC_WP_No67.

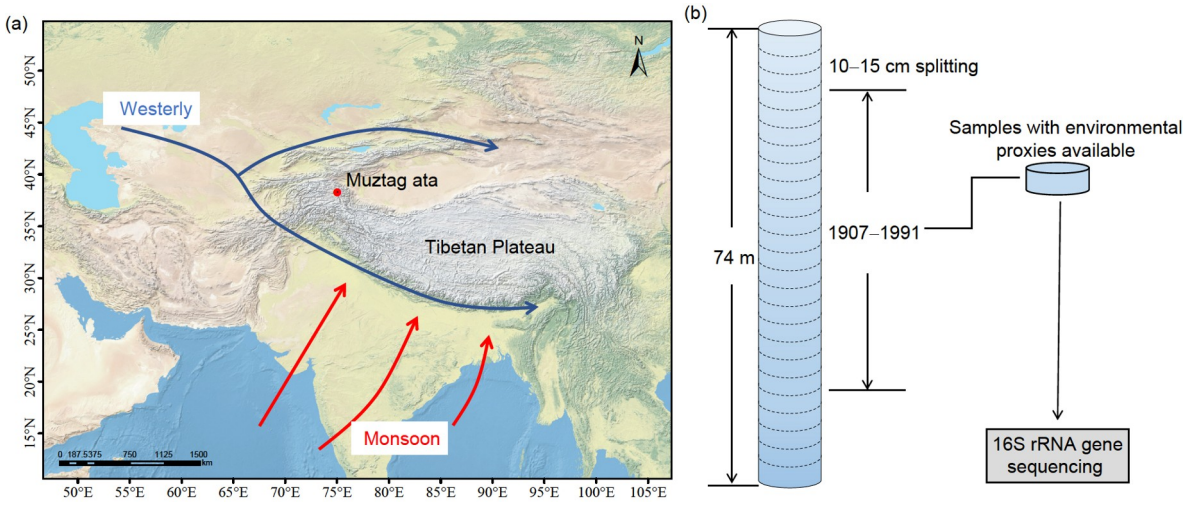

Figure 1 The location of Muztag ata glacier and the ice core sampling strategy. The location of Muztag ata glacier on the Tibetan Plateau and the influence of Westerly jet and Indian monsoon are shown in panel a. The ice core sampling strategy is illustrated in panel (b). Briefly, the 74 m ice core was cut into 10 to 15 cm sections and dated, then sections with environmental proxies available are used for DNA extraction and bacterial 16S rRNA gene amplicon sequencing.

pdf. As a complete set of environmental proxies was available for the period between 1907 and 1991, only the DNA in the ice core corresponding to this period was extracted for molecular analysis.

2.3 Bacterial molecular analysis

Approximately 300 mL of ice core was melted in the dark at a temperature of 4°C. Meltwater was filtered through 0.1 μm pore-size polycarbonate membrane filters (25 mm diameter; Millipore). The membrane filters were stored at −80°C in the laboratory until DNA extraction. Community DNA was extracted for samples with available environmental proxies (i.e., from 1907 to 1991) using the FastDNA®Spin kit (MP Biomedicals, Santa Ana, CA) according to the manufacturer's instructions. The extracted DNA was dissolved in 100 μL TE buffer and quantified by using a NanoDrop 1000 Spectrophotometer (Thermo-Scientific). The extracted DNA was stored in a −80°C refrigerator until use.

The universal primer pair 515F (5′-GTG YCA GCM GCC GCG GTA-3′) and 806R (5′-GGA CTA CHV GGG TWT CTA AT-3′) was used to amplify the V4 region of the bacterial 16S rRNA gene (Caporaso et al., 2012). The PCR products were sequenced on the MiSeq platform (Illumina Inc., San Diego, CA, USA) with paired-end strategy (2× 250 bp). The raw sequence data were processed using the USEARCH v11(Edgar, 2010) pipeline, with phylotypes clustered at 97% identity. The sequences were classified using the Bayesian classifier against the Silva database (release 128), and non-bacterial sequences were removed. After phylotype tables were constructed, samples were randomly sub-sampled without replacement to an equal depth of 12,519 to ensure that alpha diversity indices were calculated on the same sequencing depth. The raw sequencing reads generated have been deposited in the NCBI Sequence Read Archive under project ID PRJNA884890.

2.4 Multivariant and statistical analyses

The association among the environmental proxies was investigated using the Empirical Orthogonal Function (EOF) analyses performed on the scaled raw data with the wql package in R (Jassby and Cloern, 2017). The Shannon diversity, richness (number of phylotypes), and evenness indices were calculated from the rarefied phylotype table using Primer-E V6 (Clarke and Warwick, 2006). Regression analyses were performed to estimate the relationships of the bacterial diversity indices (both richness and evenness) with environmental proxies (MAP, levoglucosan, DOC, rBC, SO_4^{2-}, NH_4^+, NO_3^-, Na^+, K^+, Mg^{2+}, Ca^{2+}, Cl^-, and $\delta^{18}O$) using sigmaplot v12.5 (Systat Software, San Jose, CA) and visualized in Origin (Origin, Version 2018, OriginLab Corporation, Northampton, MA, USA). Both the linear and quadratic relationships were tested between the diversity indices and environmental proxies.

The contributions of the EOFs to the bacterial richness and evenness were explored using the Structural Equation modelling (SEM) with the Partial Least Squares Path Modeling method. The SEM analysis was performed using the plspm package in R (Sanchez et al., 2013). All environmental proxies and bacterial diversity indices were log-transformed, the associations between EOFs with bacterial indices were treated as the inner model, while the associations between environmental proxies and EOFs were treated as the outer model. The quality of the model was assessed based on the goodness-of-fit index and the *P*-values of the

structural regression results.

The trend for richness and evenness was estimated using a quasi-poisson generalized additive model (GAMs). The GAM equation can be expressed as follows:

$$g(\mu) = \theta + f_1(x_1) + f_2(x_2) + \cdots + f_n(x_n), \quad (1)$$

where g is a link function, μ is a response variable, θ is a constant, f_i, i=1, 2, …, n, is the smoothing functions of predictor variables, with a specified parametric or nonparametric form, x_i are the predictor variables.

The thin plate spline shrinkage function was chosen as the smoothing function of variables. The shrinkage methods allow unimportant effects to have their edf go to 0, simplifying predictor variables in the estimation process. The impact of the increased complexity was magnified (using "gamma=1.2") to provide slightly smoother results (Wood, 2017). The optimal smoothing parameters were selected based on the deviance explained (Yang et al., 2020). A p-value was calculated from an approximate F-test to assess the statistical significance of the effect given the other effects in the model. All GAM analyses used the "mgcv" package in R (Wood, 2017).

The bacterial community abundance matrix was aggregated to the family-level, and Hellinger transformed. A Bray-Curtis similarity matrix was then generated and hierarchical clustering was performed using complete linkage to identify the clustering pattern of samples across the ice core. Principle Coordination Analysis was also performed to visualize the community structure differences and the association of bacterial families (indicative bacterial families) with the sample variations. The relationship of livestock numbers with the relative abundance of indicative bacterial families was established using a multiple linear regression model in R (R Core Team, 2018). The best model was selected using a forward selection method based on the Akaike Information Criterion.

The dominant phylotypes (account for at least 10% of the family by relative abundance) of the indicative bacterial family were further annotated at a lower taxonomic level using EzBioCloud (Yoon et al., 2017). The proportion of bacterial community structure variation across the ice core was explained by the measured environmental proxies using distance-based linear modelling (DistLM) with the forward selection method (Legendre and Anderson, 1999) using PRIMER-E v6 (Clarke and Warwick, 2006). The significance of the fit was tested using permutations (n=999) allowing significance to a level of P=0.001. Distance-based redundancy analysis (dbRDA) ordination plots were used to visualize the associations between bacterial communities and the measured environmental proxies (Legendre and Anderson, 1999). Then, Variation partitioning analysis (VPA) based on DistLM analysis was used to partition the relative contributions of individual environmental proxy (Legendre and Anderson, 1999).

3. Results

3.1 Patterns of the measured environmental and human activities proxies in the ice core

The ice core was analyzed for environmental proxies and climate factors (including levoglucosan, DOC, rBC, SO_4^{2-}, NH_4^+, NO_3^-, Na^+, K^+, Mg^{2+}, Ca^{2+}, Cl^-, $\delta^{18}O$, and MAP). Among these proxies, rBC, NH_4^+, MAP, and levoglucosan generally increased with the year of deposition, and conversely, K^+, Mg^{2+}, Ca^{2+}, and Cl^- decreased (Figure S1 and S2). Furthermore, rBC, Na^+, Mg^{2+}, Ca^{2+}, Cl^-, SO_4^{2-}, and NO_3^- were better fitted with parabolic relationships with the R^2 values at least doubled (Appendix Table S1, https://link.springer.com). The turning points for these proxies were generally in the 1950s.

Empirical Orthogonal Function (EOF) analysis revealed the potential associations among environmental proxies, clustering them into categories. The first five EOFs explained 84% of the total variations, with EOF1 accounting for 42.1%, and being predominately loaded with soluble ions including Na^+, K^+, Mg^{2+}, Ca^{2+}, Cl^-, SO_4^{2-}, and NO_3^- (Table S2). EOF2 explained an additional 20.2% of the total variations, and was loaded with levoglucosan, rBC, and NH_4^+. Subsequently, EOF3, EOF4, and EOF5 explained 7.9%, 7.2%, and 6.8% of the variations, and were loaded with $\delta^{18}O$, MAP, and DOC, respectively.

3.2 Bacterial diversity patterns

Bacterial richness significantly increased with the year of deposition, exhibiting a positive correlation with NH_4^+, but a negative correlation with K^+ (Figure 2a and 2c). Meanwhile, the evenness showed no significant correlation with the year of deposition, though it demonstrated negative correlations with DOC and MAP, and positive correlation with $\delta^{18}O$, Na^+, K^+, Mg^{2+}, Ca^{2+}, Cl^-, SO_4^{2+}, and NO_3^- (Figure 2b and 2c). Structural Equation Modelling (SEM) was conducted to reveal the contributions of environmental proxies (Figure 3) to bacterial proxies (i.e., bacterial richness and evenness). The results indicated that only 9.3% and 20.5% of the variations in bacterial richness and evenness were explained, respectively. For the richness, its variation was significantly explained by EOF2 with a path coefficient of 0.25. The bacterial evenness was significantly explained by EOF1 only, with a path coefficient of 0.27. We then mathematically quantified the richness and evenness trends using the gen-

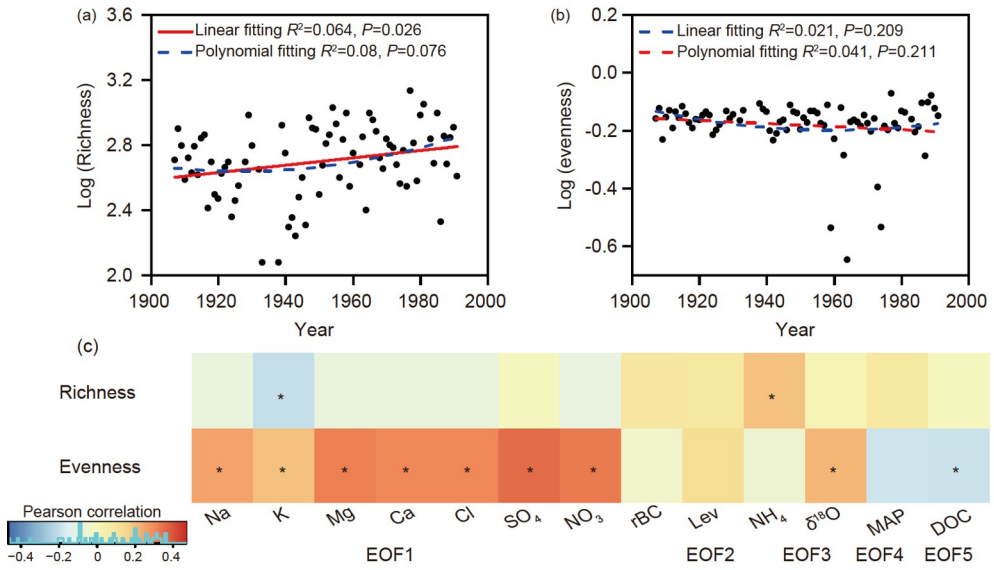

Figure 2 Patterns of bacterial richness and evenness across the ice core. The linear regression between bacterial richness (a) and evenness (b) with the dated ice core age is shown. (c) shows the correlation between bacterial richness and evenness with the measured environmental proxies. Significant correlations (at P<0.05) are marked with asterisks. rBC, refractory black carbon; MAP, mean annual precipitation; DOC, dissolved organic carbon.

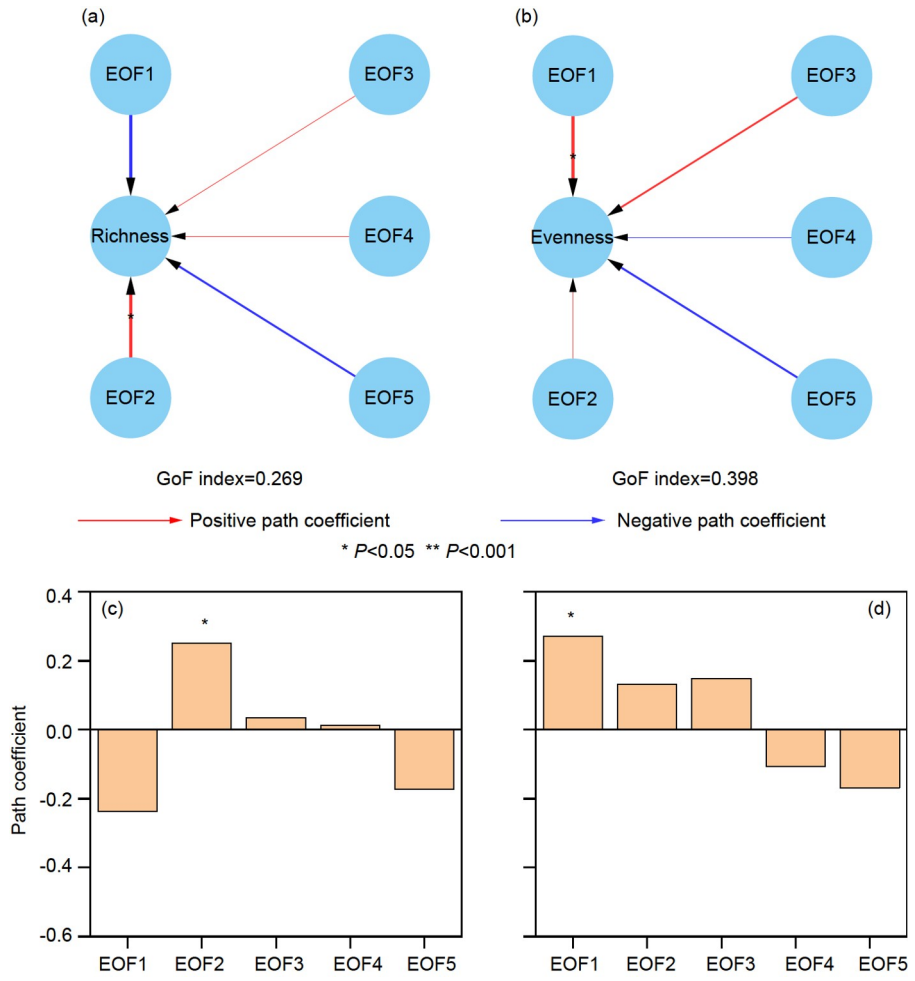

Figure 3 Structural equation modelling of bacterial richness (a) and evenness (b) in the Muztag ata glacier ice core. The path coefficients for the bacterial richness and evenness are shown in (c) and (d), respectively.

eralized additive models as equations 1 and 2 with adjusted R^2 values of 0.139 and 0.285, respectively (both $P<0.001$).

$$\text{Equation 1 : Richness} = e^{6.31855-0.0688\times \text{EOF9}+s(\text{EOF2})_{1.609}+s(\text{EOF4})_{2.522}}, \quad (2)$$

$$\text{Equation 2 : Evenness} = e^{-0.40327-0.01348\times \text{EOF1}+s(\text{EOF5})_{7.078}}. \quad (3)$$

3.3 Bacterial composition patterns

Cluster analysis of the bacterial community at the family level revealed three distinct clusters (Figure 4a). Cluster A was situated at the basal position, while Clusters B and C split at approximately 75% dissimilarity threshold. Cluster A consisted of 29 samples ranging in age from 1953 to 1991, and was further divided into two subclusters at a 65% dissimilarity threshold, with no discernible pattern based on ice core age. Cluster B comprised 11 samples from 1933 to 1951, while Cluster C comprised 37 samples from a wide range of chronological periods, the majority of which were

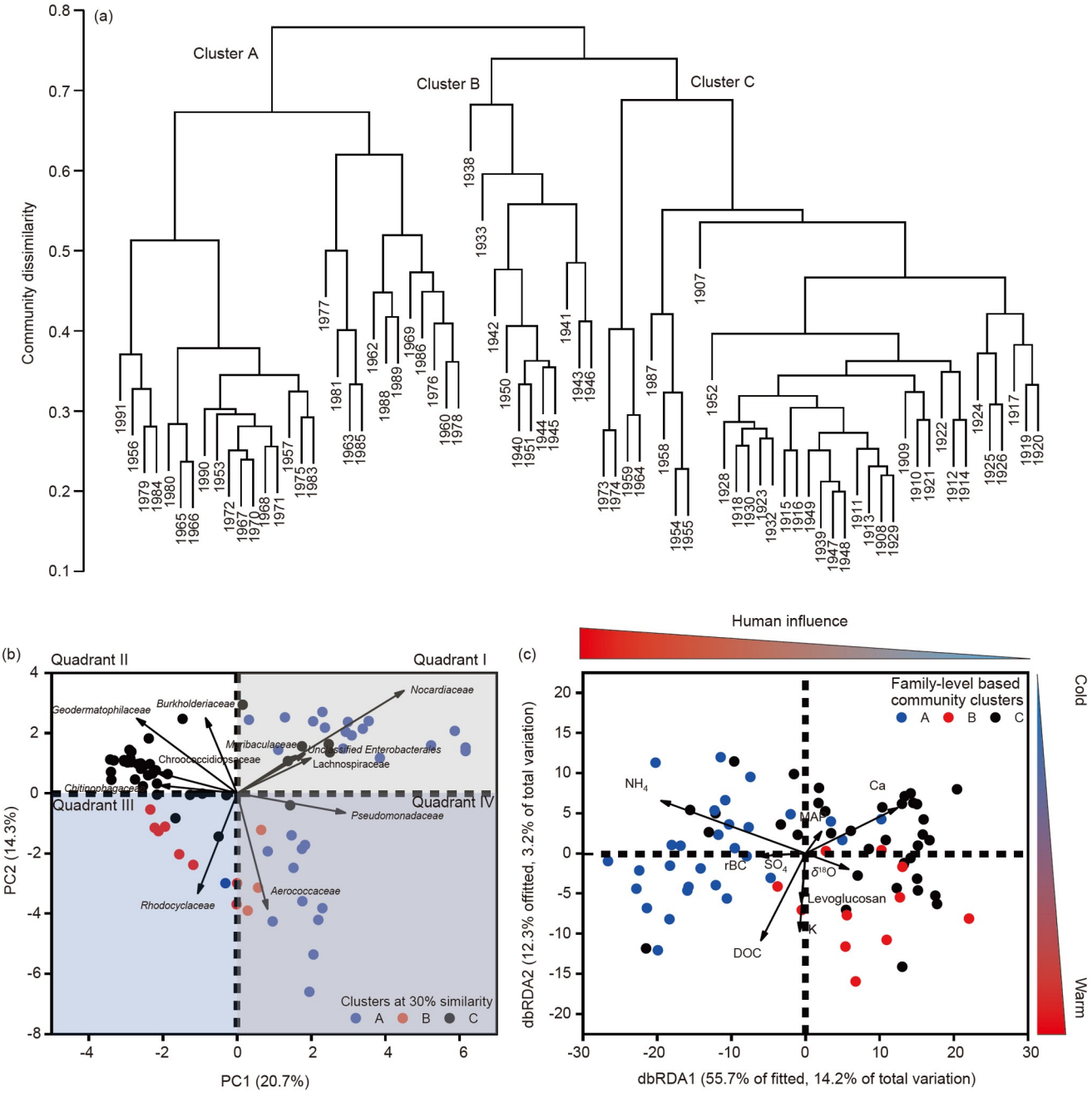

Figure 4 Community structure of bacterial community in the Muztag ata glacier. The community structure variations are visualized based on the Bray-Curtis dissimilarity of bacterial community at the family-level, following Hellinger transformation. Panel (a) shows the hierarchical clustering using complete linkage approach, panel (b) shows the principal component ordination plot with the quadrants labelled, panel (c) shows the distance-based linear modelling results and the axes are labelled based on human influence (inferred from NH_4^+ and rBC patterns) and temperature (inferred from $\delta^{18}O$ pattern).

from 1907 to 1930.

Principal component analysis revealed that Cluster A samples predominantly located in quadrants I and IV, Cluster B samples in quadrant III, and Cluster C samples in quadrant II (Figure 4b). Statistical testing indicated that samples in Quadrant I were enriched with *Nocardiaceae*, *Muribaculaceae*, and *Lachnospiraceae*; Quadrant II samples with *Burkholderiaceae*, *Geodermatophilaceae*, *Chroococcidiopsaceae*, and *Chitinophagaceae*; Quadrant III samples with *Rhodocyclacea*e; and quadrant IV samples with *Pseudomonadaceae* and *Aerococcaceae*. Dominant bacterial phylotypes (defined as having a relative abundance ≥ 10% within the family) were further annotated for pathogenicity (Table S3). Phylotypes of the genera *Ralstonia* (*Burkholderiaceae*), *Rhodococcus* (*Nocardiaceae*), *Aerococcus* (*Aerococcaceae*), and *Pseudomonas* (*Pseudomonadaceae*) were identified as potential pathogens.

The total relative abundances of *Aerococcaceae*, *Nocardiaceae*, *Muribaculaceae*, and *Lachnospiraceae* were used to reflect livestock (cattle and sheep) number changes. A dramatic increase was observed for both the relative abundance of these indicative species and the total livestock number after the 1950s (Figure 5a), with the average values increased by 1.12- and 9.17-fold, respectively. Additionally, we observed 34 consistent changes (increase or decrease) among consecutive years (61% of all instances), with a significant linear correlation being obtained between the relative abundance of these indicative species with livestock numbers (R^2=0.446, P<0.001, Figure 5b). We then used multiple linear regression to establish the relationship between the relative abundance of the enriched bacterial families (Figure 4b and Table S4) with livestock numbers. The livestock number can be expressed by the relative abundances of *Aerococcaceae*, *Nocardiaceae*, *Chitinophagaceae*, *Geodermatophilaceae*, and *Rhodocyclaceae* (Equation 3), with an adjusted R^2 of 0.558 ($F_{(5,51)}$=15.16, P<0.001).

$$\begin{aligned}\text{Equation 3}: \ \text{Log}^{(\text{Livestock number})} = & \\ -0.095 \times \log^{(1+\text{Chitinophagaceae\%})} & \\ -0.0637 \times \log^{(1+\text{Geodermatophilaceae\%})} & \\ +0.0796 \times \log^{(1+\text{Nocardiaceae\%})} & \\ +0.0849 \times \log^{(1+\text{Aerococcaceae\%})} & \\ -0.977 \times \log^{(1+\text{Rhodocyclaceae\%})} + 2.0193, & \quad (4)\end{aligned}$$

db-RDA analysis was used to explain the community composition variations attributable to environmental proxies across the ice core (Figure 4c). The measured environmental proxies accounted for 25.6% of total bacterial community variations (Table S5), with NH_4^+, DOC, and $\delta^{18}O$ exhibiting the greatest explaining power, accounting for 16.7% of the total bacterial community variations. Of the three clusters, Cluster A samples (spanning from 1953 to 1991) exhibited the highest rBC and NH_4^+, but the lowest K^+ (Figures S3 and S4); Cluster B samples (1933 to 1951) appeared to be in a transitional state between Clusters A and C, displaying environmental proxy similarities to both. For instance, rBC and NH_4^+ were similar for samples in Clusters B and C, which were both significantly lower than Cluster A samples. Cluster B samples also had similar DOC and levoglucosan as Cluster A samples, which were both higher than Cluster C samples. Lastly, Cluster C samples (1907 to 1930) had the lowest DOC and levoglucosan.

4. Discussion

4.1 Patterns of bacterial diversity, and community structure in the Muztag ata ice core

Bacterial richness was significantly higher in the more recently formed ice (Figure 2a) with a positive correlation with NH_4^+ (Figure 2c), which serves as a proxy for agricultural activity (Schwikowski et al., 1999). This suggests that enhanced agricultural activity in Central Asia could be responsible for increased bacterial richness in the Muztag ata glacier. Agricultural activities such as tillage application can facilitate soil bacterial aerosolization, while the application of fertilizer, particularly manure fertilizer, can further enhance aerosolized soil bacteria (Thiel et al., 2020).

The proportion of richness and evenness explained by environmental proxies was relatively low (9.35% and 20.5%, respectively), suggesting that the measured environmental proxies were insufficient to explain the bacterial community variations in the ice core. Bacterial aerosol transportation (Fernandez et al., 2019) and post-depositional selection (Xiang et al., 2009) may alter the bacterial community before they are frozen in the ice core. As none of these processes can be quantified accurately, this hinders the use of bacterial proxies to reflect the past climate and human activities. In contrast to chemical proxies (such as the rBC) that rarely change after being deposited on the glacier surface, several studies have reported bacterial activity on the glacier surface (Hell et al., 2013; Chen et al., 2022). This further weakens the association between bacterial proxies and environmental proxies. Nevertheless, significant correlations between bacterial diversity and environmental proxies have been reported in the present and previous studies (Miteva et al., 2009; Zhang et al., 2017). This suggests that additional studies on the dispersal and post-depositional selection processes are needed to fully utilize microbial proxies for past climate reconstruction.

Ice core samples are segregated into three distinct clusters according to their bacterial community similarity (Figure 4a), samples from the same cluster are likely to be originated from similar ecosystems with comparable climate and hu-

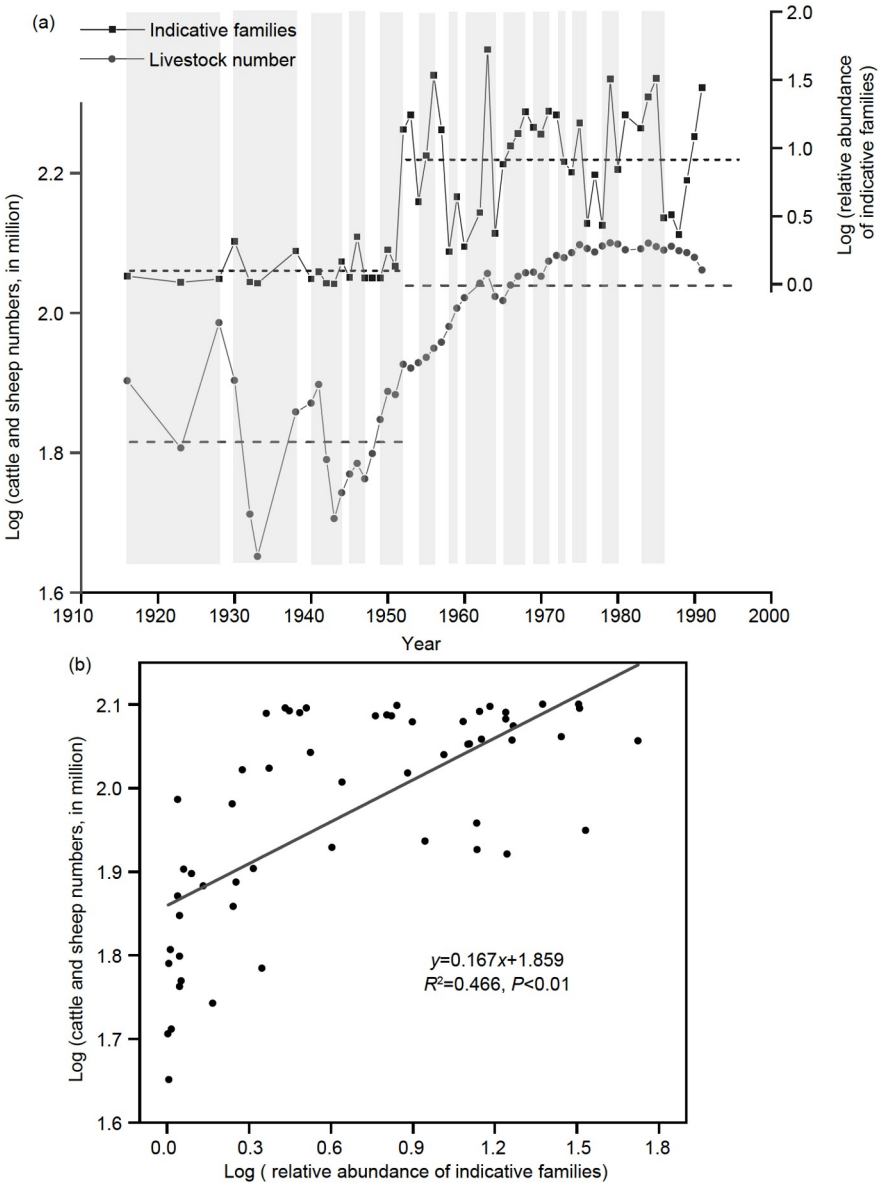

Figure 5 The associations of gut-associated microorganisms and the livestock numbers. Panel (a) shows the annual changes in the relative abundance of animal husbandry indicative lineages (*Aerococcaceae*, *Nocardiaceae*, *Muribaculaceae*, and *Lachnospiraceae*) and animal stock numbers (cattle and sheep) across the ice core. Panel (b) shows the Pearson correlation between the relative abundance of indicative lineages and animal stock numbers. For panel (a), grey areas represent the consistent year-to-year changing patterns (increase or decrease). The average value before and after 1950 was labelled with dashed lines. Animal stock numbers were obtained from the Russian Agricultural Statistics at https://www.ier.hit-u.ac.jp/rrc/English/pdf/RRC_WP_No67.pdf.

man activity strength (Romdhane et al., 2022). The greatest changes in bacterial community structure occurred after the 1950s. db-RDA plot revealed that post-1950s samples (Cluster A) were associated with increased concentrations of both NH_4^+ and rBC (Figure 4c and S4). NH_4^+ is a proxy for agricultural activity (Schwikowski et al., 1999), while rBC has been suggested to originate from open fires, energy related combustion of biomass, and fossil fuel combustion (Wang et al., 2015). An early study on the ice core from the same glacier found that the increased rBC after the 1950s was due to the increased agriculture burning during cropland expansion, which was followed by the anthropogenic black carbon emission beginning in the 1960s (Wang et al., 2015). Both these activities are considered anthropogenic, thus the substantial changes in bacterial community structure post-1950s may have been driven by human-related activities. Furthermore, the higher explanatory power of NH_4^+ compared to rBC implies that agricultural activities likely played a greater role than industrial activities.

The values of K^+, rBC, and NH_4^+ in Cluster B samples were comparable to those in Cluster C samples, while DOC and levoglucosan were similar to Cluster A samples (Figure S4). This suggests that Cluster B samples may be in a transition state, which is consistent with the chronologically order of

Cluster A, B, and C samples. Additionally, samples in Cluster C were characterized by lower levoglucosan and DOC, which are proxies for wildfire (Wang et al., 2015) and nutrient input (Yao et al., 2017), respectively. This may indicate that the samples in cluster C samples (before 1930) were associated with a period of decreased frequency of wildfire, possibly prior to the Second World War (1939–1945 AD) (Wang et al., 2015). Thus, the bacterial community in ice core may be classified based on the influence of natural conditions and human activities (Figure 4c), and can be used to reflect past environmental and human activity changes.

4.2 Natural and human-activity indicative bacterial lineages in the ice core

The present study reveals bacterial lineages that are potentially indicative to human activities. These insights cannot be obtained by other environmental proxies. Specifically, within Cluster A, quadrant I samples exhibited a higher prevalence of *Nocardiaceae*, *Muribaculaceae*, and *Lachnospiraceae* (Figure 4b). These lineages encompass a broad range of bacteria, mostly notably from the gut microbiome of ruminants, such as *Nocardiaceae* that is abundant in the small intestine of cattle (Wang et al., 2022), *Muribaculaceae* that accounted for over 10% of the gut microbiome in the duodenum of Tibetan yaks (Ma et al., 2020), and *Lachnospiraceae* that was the second most abundant bacterial group in Mongolian cattle (Aricha et al., 2021).

Cluster A quadrant IV samples were enriched with *Aerococcaceae* and *Pseudomonadaceae*. Of the *Aerococcaceae* phylotypes, the majority were affiliated with the genus *Aerococcus* (Table S3). *Aerococcus* has been proposed to originate from livestock farms (Chen et al., 2020), and is recognized as emerging human pathogens (Rasmussen, 2016). *Pseudomonadaceae* encompasses a wide range of environmental and host-associated bacteria (Peix et al., 2018). Most of the dominant *Pseudomonadaceae* phylotypes were non-pathogenic, but of soil origin (Peix et al., 2018). Thus, this suggests that the association between *Pseudomonadaceae* and human activity might be due to land use changes, leading to increased aerosolization of soil bacteria.

Cluster B was enriched with *Rhodocyclaceae*, whose relative abundance increased by 32- and 56-fold compared to that in Clusters A and C, respectively. The relative abundance of this heat-tolerant lineage was found to increase by more than 3-fold to nearly 30% after a heating event in urban regions (Fang et al., 2018). Cluster B samples (1933 to 1951) corresponded to the period during the Second World War, but the underlying mechanism of the associations between *Rhodocyclaceae* and the war requires further investigations.

Cluster C samples were characterized by low human activity but strong natural inputs (Figure 4c), which enriched *Burkholderiaceae*, *Geodermatophilaceae*, *Chroococcidiopsaceae*, and *Chitinophagaceae*. These lineages are associated with dust or aerosols. For example, *Chitinophagaceae* dominated aerosol in the Mongolian Plateau, which is also influenced by the westerly as the Muztag ata glacier (Qi et al., 2022); *Burkholderiaceae* was the main component of the Kuwait dust (Al Salameen et al., 2020); *Geodermatophilaceae* was found to dominate Mediterranean dust, which originated from Africa (Iakovides et al., 2022); and *Chroococcidiopsaceae* was associated with rainfall events and can act as nuclei for the condensation and freezing of water (Morris et al., 2011), accounting for 75% of the microbiome in rainfall in French (Dillon et al., 2020). Consequently, the relative abundance of these lineages may be used as biological proxies for environmental changes, such as enhanced dust and precipitation events.

The identified indicative bacterial families provide useful markers for reconstructing the past environmental and anthropogenic activities at the source regions. For example, the relative abundance of gut-associated microorganisms (including *Nocardiaceae*, *Muribaculaceae*, *Lachnospiraceae*, and *Aerococcaceae*) exhibited similar changing patterns to the livestock number in the Central Asian region (Figure 5). The changing pattern (increase or decrease) of the relative abundance of these indicative species was similar to that of the livestock number in the Central Asia region, particularly before the 1950s. However, a drawback of using the relative abundance as a proxy was the large annual variation, which is much greater than that observed in livestock numbers. This could be due to the changes in microorganisms from other sources, such as soil, adding "extra" variations in the relative abundance of gut-associated bacteria. However, this could be mathematically corrected by adding soil bacteria into the regression between gut-associated bacteria and livestock numbers. This was evidenced by the improved R^2 from 0.45 to 0.56 by including *Chitinophagaceae*, *Geodermatophilaceae*, and *Rhodocyclaceae*, which are representative bacteria of other sources. Therefore, we propose that the relative abundance of bacterial lineages may be used as biological proxies for animal husbandry development, an important piece of information that currently can't be provided by chemical proxies.

5. Conclusion

We present here a comprehensive analysis of the temporal dynamics of bacterial communities over the course of the twentieth century in an ice core from the Muztag ata glacier. Land-use changes due to agricultural activities, such as animal husbandry, increased bacterial richness, and the relative abundance of potential emerging pathogenic bacteria deposited on the glacier surface. As such, bacterial lineages associated with the animal gut microbiome can act as in-

dicators of regional agricultural development, further advancing our understanding of regional climate and anthropogenic activities.

Acknowledgements *This study was supported by the National Key Research and Development Plans (Grant No. 2021YFC2300904), the National Natural Science Foundation of China (Grant Nos. U21A20176 and 42330410), and the Second Tibetan Plateau Scientific Expedition and Research Program (STEP) (Grant No. 2019QZKK0503).*

Conflict of interest The authors declare that they have no conflict of interest.

References

Al Salameen F, Habibi N, Uddin S, Al Mataqi K, Kumar V, Al Doaij B, Al Amad S, Al Ali E, Shirshikhar F. 2020. Spatio-temporal variations in bacterial and fungal community associated with dust aerosol in Kuwait. PLoS ONE, 15: e0241283

Anesio A M, Lutz S, Chrismas N A M, Benning L G. 2017. The microbiome of glaciers and ice sheets. NPJ Biofilms Microbiomes, 3: 10

Aricha H, Simujide H, Wang C, Zhang J, Lv W, Jimisi X, Liu B, Chen H, Zhang C, He L, Cui Y, Gao R, Aorigele C. 2021. Comparative analysis of fecal microbiota of grazing Mongolian cattle from different regions in Inner Mongolia, China. Animals, 11: 1938

Caporaso J G, Lauber C L, Walters W A, Berg-Lyons D, Huntley J, Fierer N, Owens S M, Betley J, Fraser L, Bauer M, Gormley N, Gilbert J A, Smith G, Knight R. 2012. Ultra-high-throughput microbial community analysis on the Illumina HiSeq and MiSeq platforms. ISME J, 6: 1621–1624

Chen X, Kumari D, Achal V. 2020. A Review on airborne microbes: The characteristics of sources, pathogenicity and geography. Atmosphere, 11: 919

Chen Y, Liu K, Liu Y et al. 2022. Temporal variation of bacterial community and nutrients in Tibetan glacier snowpack. The Cryosphere, 16: 1265–1280

Clarke KR, Warwick RM. 2006. PRIMER v6: User manual/tutorial. PRIMER-E, Plymouth

da C Jesus E, Marsh T L, Tiedje J M, de S Moreira F M. 2009. Changes in land use alter the structure of bacterial communities in Western Amazon soils. ISME J, 3: 1004–1011

Dillon K P, Correa F, Judon C, Sancelme M, Fennell D E, Delort A M, Amato P. 2020. Cyanobacteria and algae in clouds and rain in the area of puy de Dôme, central France. Appl Environ Microbiol, 87: e01850

Edgar R C. 2010. Search and clustering orders of magnitude faster than BLAST. Bioinformatics, 26: 2460–2461

Fang Z, Guo W, Zhang J, Lou X. 2018. Influence of heat events on the composition of airborne bacterial communities in urban ecosystems. Int J Environ Res Public Health, 15: 2295

Fernandez M O, Thomas R J, Garton N J, Hudson A, Haddrell A, Reid J P. 2019. Assessing the airborne survival of bacteria in populations of aerosol droplets with a novel technology. J R Soc Interface, 16: 20180779

Hell K, Edwards A, Zarsky J, Podmirseg S M, Girdwood S, Pachebat J A, Insam H, Sattler B. 2013. The dynamic bacterial communities of a melting High Arctic glacier snowpack. ISME J, 7: 1814–1826

Iakovides M, Tsiamis G, Tziaras T, Stathopoulou P, Nikolaki S, Iakovides G, Stephanou E G. 2022. Two-year systematic investigation reveals alterations induced on chemical and bacteriome profile of PM2.5 by African dust incursions to the Mediterranean atmosphere. Sci Total Environ, 815: 151976

Jassby A D, Cloern J E. 2017. wq: Exploring water quality monitoring data. R package version 0.4.9. https://cran.r-project.org/package=wq

Legendre P, Anderson M J. 1999. Distance-based redundancy analysis: Testing multispecies responses in multifactorial ecological experiments. Ecol Monogr, 69: 1–24

Legrand M, Mayewski P. 1997. Glaciochemistry of polar ice cores: A review. Rev Geophys, 35: 219–243

Li Z, Yao T, Tian L, Xu B, Wu G, Zhu G. 2004. Borehole temperature at the Ice-core drilling site in the Muztag Ata glacier, East Pamirs. J Glaciol Geocryol, 26: 284–288

Liu Y, Priscu J C, Yao T, Vick-Majors T J, Xu B, Jiao N, Santibáñez P, Huang S, Wang N, Greenwood M, Michaud A B, Kang S, Wang J, Gao Q, Yang Y. 2016. Bacterial responses to environmental change on the Tibetan Plateau over the past half century. Environ Microbiol, 18: 1930–1941

Ma J, Zhu Y, Wang Z, Yu X, Hu R, Wang X, Cao G, Zou H, Shah A M, Peng Q, Xue B, Wang L, Zhao S, Kong X. 2020. Comparing the bacterial community in the gastrointestinal tracts between growth-retarded and normal yaks on the Qinghai-Tibetan Plateau. Front Microbiol, 11: 600516

McConnell J R, Edwards R, Kok G L, Flanner M G, Zender C S, Saltzman E S, Banta J R, Pasteris D R, Carter M M, Kahl J D W. 2007. 20th-Century industrial black carbon emissions altered Arctic climate forcing. Science, 317: 1381–1384

Miteva V, Teacher C, Sowers T, Brenchley J. 2009. Comparison of the microbial diversity at different depths of the GISP2 Greenland ice core in relationship to deposition climates. Environ Microbiol, 11: 640–656

Morris C E, Sands D C, Bardin M, Jaenicke R, Vogel B, Leyronas C, Ariya P A, Psenner R. 2011. Microbiology and atmospheric processes: Research challenges concerning the impact of airborne micro-organisms on the atmosphere and climate. Biogeosciences, 8: 17–25

Peix A, Ramírez-Bahena M H, Velázquez E. 2018. The current status on the taxonomy of Pseudomonas revisited: An update. Infect Genet Evol, 57: 106–116

Price P B. 2007. Microbial life in glacial ice and implications for a cold origin of life. FEMS Microbiol Ecol, 59: 217–231

Price P B, Bay R C. 2012. Marine bacteria in deep Arctic and Antarctic ice cores: A proxy for evolution in oceans over 300 million generations. Biogeosciences, 9: 3799–3815

Qi J, Ji M, Wang W, Zhang Z, Liu K, Huang Z, Liu Y. 2022. Effect of Indian monsoon on the glacial airborne bacteria over the Tibetan Plateau. Sci Total Environ, 831: 154980

R Core Team. 2018. R: A language and environment for statistical computing. R Foundation for Statistical Computing, Vienna, Austria

Rasmussen M. 2016. Aerococcus: An increasingly acknowledged human pathogen. Clin Microbiol Infect, 22: 22–27

Romdhane S, Spor A, Banerjee S, Breuil M C, Bru D, Chabbi A, Hallin S, van der Heijden M G A, Saghai A, Philippot L. 2022. Land-use intensification differentially affects bacterial, fungal and protist communities and decreases microbiome network complexity. Environ Microbiome, 17: 1

Sanchez G, Trinchera L, Sanchez MG, et al. 2013. Package 'plspm'. Citeseer: State College, PA, USA

Santibáñez P A, Maselli O J, Greenwood M C, Grieman M M, Saltzman E S, McConnell J R, Priscu J C. 2018. Prokaryotes in the WAIS Divide ice core reflect source and transport changes between Last Glacial Maximum and the early Holocene. Glob Change Biol, 24: 2182–2197

Schwikowski M, Brütsch S, Gäggeler H W, Schotterer U. 1999. A high-resolution air chemistry record from an Alpine ice core: Fiescherhorn glacier, Swiss Alps. J Geophys Res, 104: 13709–13719

Thiel N, Münch S, Behrens W, Junker V, Faust M, Biniasch O, Kabelitz T, Siller P, Boedeker C, Schumann P, Roesler U, Amon T, Schepanski K, Funk R, Nübel U. 2020. Airborne bacterial emission fluxes from manure-fertilized agricultural soil. Microb Biotechnol, 13: 1631–1647

Tian L, Yao T, Li Z, Macclune K, Wu G, Xu B, Li Y, Lu A, Shen Y. 2006. Recent rapid warming trend revealed from the isotopic record in Muztagata ice core, eastern Pamirs. J Geophys Res, 111: D13103

Wang K, Zhang H, Hu L, Zhang G, Lu H, Luo H, Zhao S, Zhu H, Wang Y. 2022. Characterization of the microbial communities along the gastrointestinal tract in crossbred cattle. Animals, 12: 825

Wang M, Xu B, Kaspari S D, Gleixner G, Schwab V F, Zhao H, Wang H,

Yao P. 2015. Century-long record of black carbon in an ice core from the Eastern Pamirs: Estimated contributions from biomass burning. Atmos Environ, 115: 79–88
Wood S.N. 2017. Generalized Additive Models an introduction with R. Chapman & Hall/CRC Texts in Statistical Science. Chapman and Hall/CRC
Xiang S R, Shang T C, Chen Y, Yao T D. 2009. Deposition and post-deposition mechanisms as possible drivers of microbial population variability in glacier ice. FEMS Microbiol Ecol, 70: 165–176
Yang Y, Yi Y, Wang W, Zhou Y, Yang Z. 2020. Generalized additive models for biomass simulation of submerged macrophytes in a shallow lake, Sci Total Environ, 711:13510. Sci Total Environ, 711: 135108
Yao T, Xiang S, Zhang X, Wang N, Wang Y. 2006. Microorganisms in the Malan ice core and their relation to climatic and environmental changes. Glob Biogeochem Cycle, 20: GB1004
Yao T, Liu Y, Kang S, Jiao N, Zeng Y, Liu X, Zhang Y. 2008. Bacteria variabilities in a Tibetan ice core and their relations with climate change. Glob Biogeochem Cycle, 22: GB4017
Yao T, Masson-Delmotte V, Gao J, Yu W, Yang X, Risi C, Sturm C, Werner M, Zhao H, He Y, Ren W, Tian L, Shi C, Hou S. 2013. A review of climatic controls on δ^{18}O in precipitation over the Tibetan Plateau: Observations and simulations. Rev Geophys, 51: 525–548
Yao T, Li Z, Thompson L G, Mosley-Thompson E, Wang Y, Tian L, Wang N, Duan K. 2017. δ^{18}O records from Tibetan ice cores reveal differences in climatic changes. Ann Glaciol, 43: 1–7
Yoon S H, Ha S M, Kwon S, Lim J, Kim Y, Seo H, Chun J. 2017. Introducing EzBioCloud: A taxonomically united database of 16S rRNA gene sequences and whole-genome assemblies. Int J Systatic Evolary Microbiol, 67: 1613–1617
Zhang X, Yao T, An L, Tian L, Xu S. 2017. A study on the vertical profile of bacterial DNA structure in the Puruogangri (Tibetan Plateau) ice core using denaturing gradient gel electrophoresis. Ann Glaciol, 43: 160–166
Zhang X F, Yao T D, Tian L D, Xu S J, An L Z. 2008. Phylogenetic and physiological diversity of bacteria isolated from Puruogangri ice core. Microb Ecol, 55: 476–488
Zhao H, Xu B, Yao T, Tian L, Li Z. 2011. Records of sulfate and nitrate in an ice core from Mount Muztagata, central Asia. J Geophys Res, 116: D13304

(Editorial handling: Huayu LU)